Organic Electronics 13 (2012) 264–272

Contents lists available at SciVerse ScienceDirect

Organic Electronics

journal homepage: www.elsevier.com/locate/orgel

Large plate-like organic crystals from direct spin-coating for solution-processed field-effect transistor arrays with high uniformity

Yun Li [a], Chuan Liu [a], Akichika Kumatani [a], Peter Darmawan [a], Takeo Minari [a], Kazuhito Tsukagoshi [a,b,*]

[a] International Center for Materials Architectonics (MANA), National Institute for Materials Science (NIMS), Tsukuba, Ibaraki 305-0044, Japan
[b] Core Research of Evolutional Science & Technology (CREST), Japan Science and Technology Agency (JST), Kawaguchi, Saitama 332-0012, Japan

ARTICLE INFO

Article history:
Received 29 July 2011
Received in revised form 23 October 2011
Accepted 22 November 2011
Available online 7 December 2011

Keywords:
Small-molecule organic crystals
Plate-like crystals
Organic field-effect transistor arrays
Solution-processed
Patterning
Uniformity

ABSTRACT

Solution-processed organic crystals are important in field-effect transistors because of their highly ordered molecular packing and ease of device fabrication. For practical applications, the patterning of organic crystal transistor arrays is critical. However, uniformity, which concerns the variation in electrical performance among devices fabricated simultaneously on the same substrate, is a common consideration in the commercial applications of the solution-processed organic crystal transistor arrays. Here, a simple approach for fabricating field-effect transistor arrays based on organic plate-like crystals is reported. Through this method, a direct spin-coating process from a mixture solution of organic semiconductor and polymer dielectric can produce organic plate-like crystals. The grain size of the crystals is observed to be hundreds of micrometers. By controlling the concentrations of the active materials, the transistor arrays exhibit high uniformity and good device performance. The results presented in this work promise that this approach is a comparable technology to hydrogenated amorphous silicon-based FETs and is a great candidate for practical applications in electronic devices.

1. Introduction

1.1. Patterning of solution-processed organic crystal field-effect transistor arrays

Organic field-effect transistors (OFETs) have been the subject of intensive interest because of their potential in electronic devices [1,2]. A significant number of studies in this field have considered organic crystals as ideal materials for devices with good performance because of their highly ordered molecules. Grain boundaries and molecular disorder in amorphous or polycrystalline thin films limit the charge transport by scattering the charge carriers. The absence of these scattering centers is the principal advantage of organic crystals [3]. The reported values of carrier mobility are much higher in organic crystals than in OFETs made of polycrystalline semiconductors [4–6].

Among various materials, solution-processed organic semiconducting crystals are more appreciable because they allow for ease of device fabrication and low cost. Polymeric materials are always processed from solutions, but they are commonly exhibited in the amorphous or polycrystalline phase because of their weak molecular interaction [7–11]. Small-molecule semiconductors have good thermal and chemical stability and typically exhibit better performance than polymers. However, small-molecule semiconductors are often insoluble [12]. Thus, vapor-processing techniques in vacuum are the most commonly used for the growth of small-molecule crystals, such as rubrene, pentacene, and C_{60} [5,13,14]. Owing to the intensive efforts in the molecular design, many dissolvable small-molecule semiconducting materials that can form into crystalline phase are synthesized and developed by

* Corresponding author at: International Center for Materials Architectonics (MANA), National Institute for Materials Science (NIMS), Tsukuba, Ibaraki 305-0044, Japan.
E-mail address: TSUKAGOSHI.Kazuhito@nims.go.jp (K. Tsukagoshi).

1566-1199/$ - see front matter © 2011 Elsevier B.V. All rights reserved.
doi:10.1016/j.orgel.2011.11.012

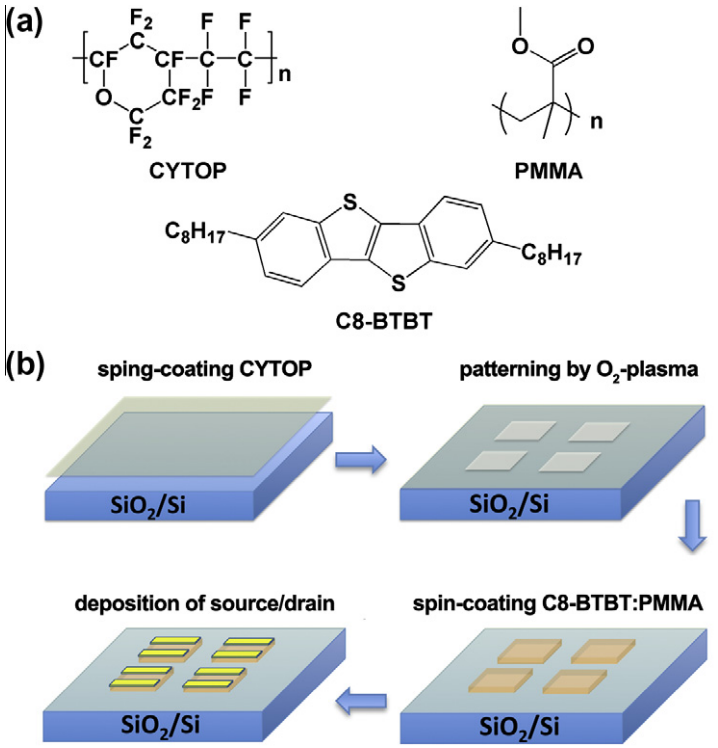

Fig. 1. (a) Molecular structures of the materials used, including CYTOP, dioctylbenzothienobenzothiophene (C8-BTBT), and polymethylmethacrylate (PMMA). (b) Fabrication process of patterning the field-effect transistor arrays based on plate-like organic crystals by using hydrophobic dielectric of CYTOP. The organic crystals are formed via a simple spin-coating process from a mixture solution of C8-BTBT and PMMA.

optimizing the relevant device architectures and parameters [15–20]. The field-effect mobility obtained is up to 9 $cm^2 V^{-1} s^{-1}$ from the devices based on solution-processed small-molecule organic crystals [20].

To turn organic crystals into a viable semiconductor technology, the patterning of organic crystal transistor arrays that allow well-defined geometric features is desirable [21–27]. Hand picking and placing the individual crystals is the most common approach, but it limits the potential applications of this method in reality and lowers the device performance because of the introduced contamination and crystal damage [28,29]. Recently, some well-developed methods, such as those introducing patterned wettability, have been reported for solution-processed organic crystal transistor arrays [27,30–36].

1.2. Uniformity of device performance of solution-processed organic crystal field-effect transistor arrays

At present, many efforts have been devoted to the improvement of the device performance of solution-processed organic crystal FET arrays. Moreover, uniformity, which concerns the variation of electrical performance among devices fabricated simultaneously on the same substrate, is also an important consideration. Even when fabricated simultaneously on the same substrate, the pattern OFET arrays often show large variations of performance. This acts as a critical limitation to practical applications, such as active matrix backplanes for electronic papers or displays [27,30,37]. Thus, the production of FET arrays based on organic crystals with high uniformity and exhibiting small variations of performance is a great challenge.

This variation of the device performance of organic crystal FET arrays can be attributed to two reasons. One reason is the orientation and alignment of the crystals, which introduce the anisotropy of charge transport and differences in the width and length of the conducting channels. The other reason is the morphology of the crystals. For instance, in our previous work, FET arrays based on rod-like organic crystals, which were formed in the patterned regions by spin-coating and solvent–vapor annealing, showed poor uniformity in electrical performance [32]. Such large variation was attributed to the difference in the quality of metal/semiconductor contact. Assuming that the amount of the active materials in each patterned region is similar, wider and longer crystals should have smaller crystal thickness. The crystal thickness determines the access resistance from the metal/semiconductor interface to the conducting channel. Consequently, the metal contact quality in organic crystal FETs is greatly influenced by the crystal shapes and sizes, which further results in the variations of performance.

1.3. Organic plate-like crystals for the application of FET arrays

Organic plate-like crystals with large grain sizes are promising candidates for FET arrays with high uniformity in device performance because they can provide more physically uniform films. Here, a simple and solution-

processed approach to pattern the surface wettability using hydrophobic dielectric and to produce large plate-like organic crystals only within the patterned regions is reported. CYTOP was spin-coated onto a SiO_2/Si substrate and then selectively exposed to the O_2-plasma to form patterned wettability. Subsequently, a direct spin-coating process without any post-treatment can produce plate-like organic crystals confined well within the patterned regions. The grain size was as large as hundreds of micrometers. Finally, by evaporating Au to form the source and drain electrodes, the transistor arrays were fabricated with a bottom-gate top-contact structure. By optimizing the concentration, the transistors exhibited good electrical performance and high uniformity. The results presented in this work prove that the proposed method is a technology comparable with hydrogenated amorphous silicon-based FETs.

2. Experimental

2.1. Device fabrication

Fig. 1a shows the molecular structures of the materials used in this work, including CYTOP (Asahi Glass), polymethylmethacrylate (PMMA, polymeric dielectric), and dioctylbenzothienobenzothiophene (C8-BTBT, p-type semiconductor). The fabrication process of the patterned OFETs is illustrated in Fig. 1b. Highly doped n-type (100) silicon wafers with 50 nm SiO_2 layers were cleaned in an ultrasonic bath in a succession of acetone and 2-propanol for 10 min each. C8-BTBT (Nippon Kayaku) and PMMA (Aldrich, M_W = 10,000) were dissolved in anisole. CYTOP (33 wt.%) was spin-coated onto the pre-cleaned SiO_2 (50 nm)/Si substrates (500 rpm for 5 s and 2000 rpm for 60 s). And then, the substrate was baked at 90 °C for 30 min for complete drying. After that, the substrate with CYTOP was covered with a shadow mask and subjected to the O_2-plasma treatment (60 W) for 5 min. The O_2-plasma treatment was performed in a reactive ion etching system supplied by Yamato Corporation. This treatment resulted in partial removal of the hydrophobic CYTOP layer and the formation of highly hydrophilic regions with a contact angle of less than 5°. The size of patterned squares is 0.5×0.2 mm^2 with the depth of ~40 nm. Besides, for FTS-patterned samples, UV–ozone treatment was taken by a photo surface processor (Model: PL16-200-3, Sen Lights Corporation) for 3 min with a low-temperature Hg lamp power supply (Model: UVE-200J, Sen Lights Corporation). After the patterning of surface wettability, the mixture solution of C8-BTBT and PMMA in anisole was spin-coated onto the substrates (500 rpm for 5 s and 4000 rpm for 200 s). Due to the wettability difference, small droplets were confined in the square regions without CYTOP coating after this spin-coating process. It resulted in selective deposition in desired geometry. Hence, the individual devices were isolated from each other. Finally, MoO_X and Au are thermally evaporated subsequently through a shadow mask to form the source and drain electrodes. And the devices exhibited as the bottom-gate top-contact structure.

2.2. Surface patterning, crystal and device characterization

The microscope images of organic crystals were collected by using Olympus BX51. And the microscope images showing the crystals at different rotatory degrees were taken by Nikon Eclipse LV100POL. A standard surface profiler (Model P-16, KLA Tensor) was applied to measure the film thickness and the depth of patterned regions. A contact angle goniometer developed by Imoto Corporation was used to examine the surface wettability with water (18 MΩ cm) as the sessile drop for all samples. The FET arrays were measured under vacuum ($<3 \times 10^{-4}$ Pa) using an Agilent 4156C semiconductor parameter analyzer.

3. Results and discussion

3.1. Patterning the surface wettability

A perfluorinated polymer of CYTOP (33 wt.%) was spin-coated onto the pre-cleaned SiO_2 (50 nm)/Si substrate. The substrate was then baked at 90 °C for 30 min for the complete drying of the solvent. The CYTOP film is a very hydrophobic fluoropolymer with a water contact angle of ~105° (as shown in Fig. 2c) [38]. After that, the substrate with

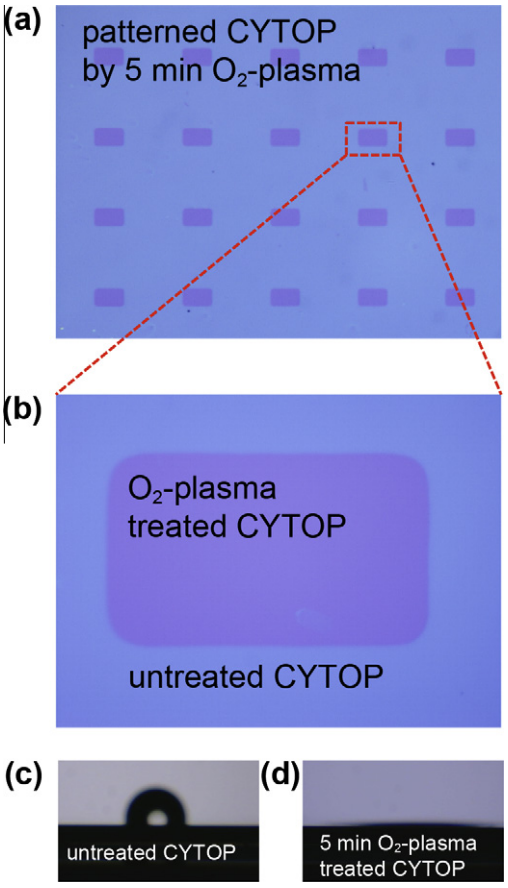

Fig. 2. (a) and (b) Show the microscope images of the CYTOP film with patterned arrays after 5 min of the O_2-plasma treatment. (c) and (d) Show the images of the water contact angles for an untreated CYTOP surface and that after 5 min of the O_2-plasma treatment, respectively.

CYTOP was covered with a shadow mask and subjected to the O_2-plasma treatment. The O_2-plasma treatment lasted for 5 min, and thus the contact angle of the surface dramatically decreased to less than 5° (Fig. 2d). This treatment resulted in the partial removal of the hydrophobic CYTOP layer, and a surface with patterned wettability exhibiting geometry in good accordance with the shadow mask (Fig. 2a and b). The size of the patterned squares was 0.5×0.2 mm^2, and the depth was ~40 nm, as measured using a surface profiler. Since the thickness of the CYTOP layer was ~75 nm, 5 min of the O_2-plasma treatment could not reach the surface of SiO_2/Si substrate and leaving a relatively thinner layer of CYTOP.

3.2. Plate-like organic crystals observations

C8-BTBT is a promising and dissolvable organic semiconducting small molecule that can present good device performance in OFETs. Using different deposition techniques and post-deposition treatments, C8-BTBT can exhibit the polycrystalline phase [30,31,39] or form into rod-like crystals [20]. One interesting property of the proposed approach is that a simple and direct spin-coating process from a mixture solution of C8-BTBT and PMMA can produce thin films consisting of large C8-BTBT plate-like crystals. A double layer, with PMMA underneath C8-BTBT, was formed because of phase separation, which is consistent with the result of a previous study [20].

Table 1
C8-BTBT and PMMA concentrations for sample groups I–V.

Sample group	I	II	III	IV	V
C8-BTBT concentration (wt.%)	1.0	0.5	0.5	0.5	0.2
PMMA concentration (wt.%)	2.0	1.0	0.5	0.2	0.2

By fabricating five sample groups (i.e., I–V, Table 1), the material concentration was found influence the formation and morphology of the plate-like crystals. As shown in Fig. 3a–d and f–j, when the concentrations of C8-BTBT and PMMA were relatively higher (sample groups I–IV), crystals with grain sizes of hundreds of micrometers were observed in the patterned regions. The crystals showed strong birefringence in optical micrographs recorded under cross-polarized light, confirming their crystalline nature. Fig. 3k shows typical C8-BTBT crystals, as highlighted by the red dotted square in Fig. 3h. The angle of facets at the crystal front end is ~104°, consistent with the angle between crystal planes (1 1 0) and 1 $\bar{1}$ 0 (106°) [20,40].

Fig. 3l shows the cross-polarized images of the crystals at the channel region, as highlighted by the red dotted square in Fig. 3i, with the substrate rotated at different degrees. In Fig. 3i, several large organic crystals were observed in the

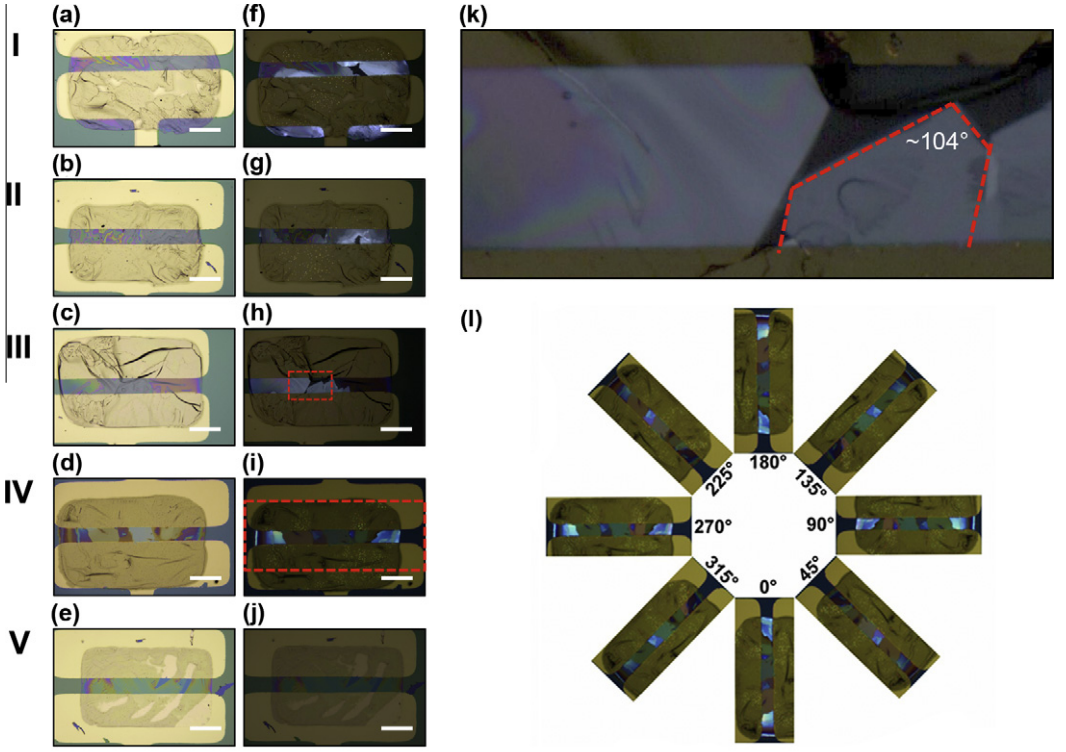

Fig. 3. (a)–(e) Show the microscope images of the typical patterned regions after the deposition of source and drain electrodes for sample groups I–IV, respectively. (f)–(j) are the cross-polarized microscope images in accordance with (a)–(e), respectively. (k) Shows the crystals in the red-dotted square in (h), with the angle of facets at the crystal front end is ~104°, consistent with the angle between the crystal planes 1 1 0 and 1 $\bar{1}$ 0 (106°). (l) Cross-polarized microscope image of the plate-like organic crystals within the red-dotted square in the channel region of (i), with the substrate rotated at different degrees. The scale bars in (a)–(j) are for 100 nm in length. (For interpretation of the references to color in this figure legend, the reader is referred to the web version of this article.)

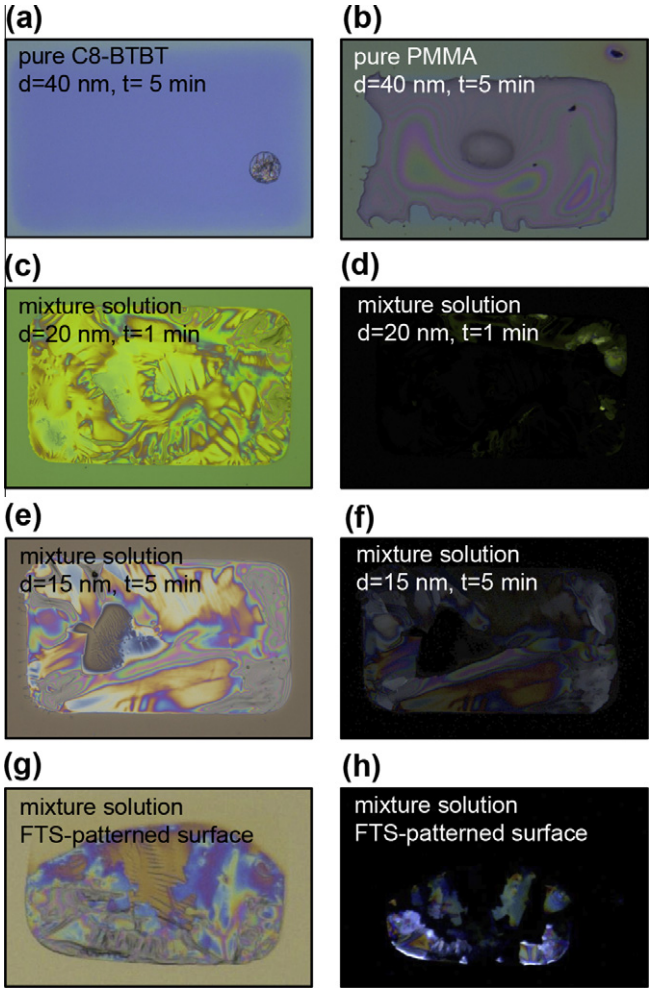

Fig. 4. (a) and (b) are the bright-field microscope images of the polycrystalline C8-BTBT small dots in the patterned region after spin-coating a pure C8-BTBT solution (0.5 wt.%) and a pure PMMA solution (0.5 wt.%), respectively. (c) and (d) Show the bright-field and cross-polarized microscope images of an as-spun film from a mixture solution of C8-BTBT (0.5 wt.%) and PMMA (0.5 wt.%) on the surface patterned by CYTOP with 1 min of the O_2-plasma treatment. The depth of the patterned region is ~20 nm. (e) and (f) are the bright-field and cross-polarized microscope images of the film on the substrate with a relatively thinner CYTOP layer treated with 5 min of the O_2-plasma treatment, respectively. The depth of the patterned region is ~15 nm. (g) and (h) are the bright-field and cross-polarized microscope images of a film from a C8-BTBT/PMMA solution on the substrate, the wettability of which is patterned by applying self-assembled molecules of (tridecafluoro-1,1,2,2-tetrahydrooctyl)trichlorosilane (FTS). The film exhibits the polycrystalline phase. In (a)–(f), *d* and *t* represent the depth of the patterned region and the duration of the O_2-plasma treatment, respectively.

channel region. In Fig. 3l, each of these crystals changed its color simultaneously during rotation. It indicates that each crystal is assembled with the same crystal orientation. However, Fig. 3e and j show that lower concentrations of C8-BTBT (0.2 wt.%) and PMMA (0.2 wt.%) produced an as-spun film of amorphous C8-BTBT with no crystallinity, which could be attributed to the fact that a lower concentration results in a larger distance among C8-BTBT molecules than that with strong molecular interaction for the formation of crystals. Moreover, the material concentration has critical influences on electrical performance, especially on device uniformity, which will be discussed later.

3.3. Discussion on the formation of C8-BTBT plate-like crystals

A similar patterning process using hydrophobic dielectric was also applied for polycrystalline triisopropylsilylethynyl pentacene (TIPS-PEN) transistors with a crystallization-assisting layer of hexamethyldisilazane [38]. In the proposed method, the formation of organic plate-like crystals is determined by the addition of PMMA into the C8-BTBT solution and the influence of the CYTOP sidewalls at the edges of patterned regions. As reference to the C8-BTBT plate-like crystals, C8-BTBT films formed through the spin-coating process from the anisole solution in the absence of any PMMA adopt small polycrystalline dots in the middle region of the patterned areas (Fig. 4a). The formation of small polycrystalline dots suggests strong molecular interaction of the C8-BTBT molecules. In comparison, a pure PMMA solution formed a physically more uniform film in the patterned region (Fig. 4b). Considering the plate-like crystals obtained from the mixture solution of C8-BTBT and PMMA, it could be deduced that PMMA was well spread in the patterned region along with the C8-BTBT

molecules, preventing the shrinking of C8-BTBT into small dots.

To investigate further the formation of plate-like crystals, the mixture solution of C8-BTBT (0.5 wt.%) and PMMA (0.5 wt.%) was spin-coated onto patterned CYTOP-coated substrates with thinner CYTOP sidewalls. In Fig. 4c and d, the CYTOP layer was patterned by the same shadow mask but had a shorter time for the O_2-plasma treatment (1 min), resulting in a thinner CYTOP sidewall of 20 nm. Much smaller plate-like crystals could only be observed in the regions close to the edges of the patterned region. The differences in the crystal size and orientation could be due to the height of the CYTOP sidewall.

The O_2-plasma treatment time also has an influence on the wettability of the surface. Consequently, a CYTOP layer was spin-coated from the solution with a lower concentration (9 wt.%). The substrate was subjected to the O_2-plasma treatment for 5 min. This treatment was also incapable of removing the entire CYTOP layer in the patterned region, giving similar wettability. The resulting patterned regions had CYTOP sidewalls with a height of ~15 nm. By spin-coating from the C8-BTBT/PMMA solution with the same concentration, the resulting film also comprised relatively smaller plate-like crystals close to the edges of the patterned region compared with the crystals in a patterned region with higher CYTOP sidewalls (Fig. 4e and f). Furthermore, the SiO_2/Si surface was also patterned by using a self-assembled molecule material of (tridecafluoro-1,1,2,2-tetrahydrooctyl)trichlorosilane (FTS). The wettability was patterned by using a shadow mask under the UV–ozone treatment for 5 min. Consequently, the height of the sidewalls of the patterned regions was at the level of the molecular length (1–2 nm). The patterned region was highly hydrophilic, with a contact angle of ~7°, close to that of a CYTOP-patterned surface. However, a polycrystalline film formed in the patterned regions by spin-coating from the C8-BTBT/PMMA solution (Fig. 4g and h). Therefore, based on these results, the formation of C8-BTBT plate-like crystals can also be attributed to the influence of the CYTOP sidewalls at the edges of the patterned regions on the amount of the solution within the patterned regions during spin-coating and/or on the enhancement of the PMMA spreading.

Consequently, the formation of plate-like organic crystals was stimulated by the strong molecular interaction and large-distance movement of the C8-BTBT molecules, with the assistance of the PMMA spreading on the surface of the patterned regions (Fig. 5). The hydrophobic CYTOP sidewall at the edges of the patterned regions can enhance the spreading of PMMA. The influence of the height of the CYTOP sidewall is of interest and is still under investigation. Besides, anisole used in this work is a high-boiling point solvent (boiling point = 154 °C) that enables slow solvent evaporation during the spin-coating process, resulting in a thermodynamically preferred crystalline structure.

3.4. Measuring the transistor behavior

In sample groups I–IV, similar crystal shapes and sizes in the patterned regions were observed, while device performance was greatly influenced by the material concentrations. The transfer and output curves of the C8-BTBT plate-like crystal OFETs fabricated from sample groups I–IV are shown in Fig. 6. The μ_{FET} and V_{th} values are calculated in the saturation regime using the following equation [41]:

$$I_D = \frac{W}{2C_iL}\mu_{FET}(V_G - V_{th})^2, \quad (1)$$

where W and L are the width and length of the channel, respectively, and C_i is the capacitance per unit area of the gate dielectric. The average thickness of PMMA underneath the C8-BTBT crystals was measured as 30, 10, 8 and 6 nm for sample groups I–IV, respectively. As shown in Fig. 6a, the devices with different material concentrations all showed typical field-effect transistor behavior. The average μ_{FET} from sample groups I–IV increased from 0.02, 0.04,

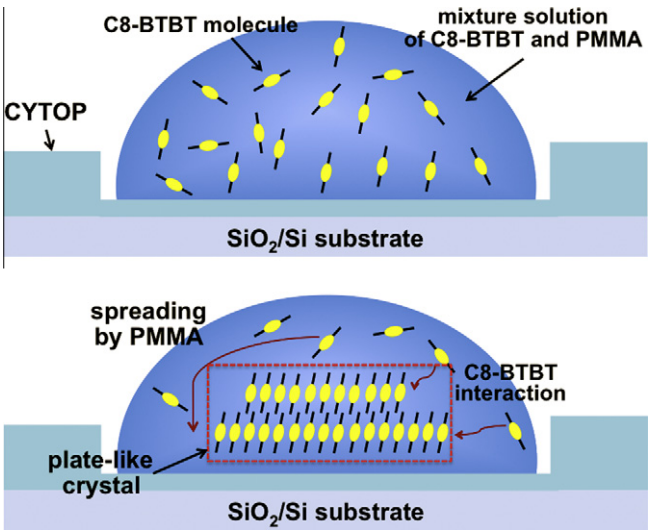

Fig. 5. Illustrative representation of the mixture solution on the surface of the patterned region, showing that the formation of plate-like organic crystals can be attributed to the strong molecular interaction and large-distance movement of C8-BTBT molecules, with the assistance of the PMMA spreading on the highly hydrophilic surface of the patterned regions.

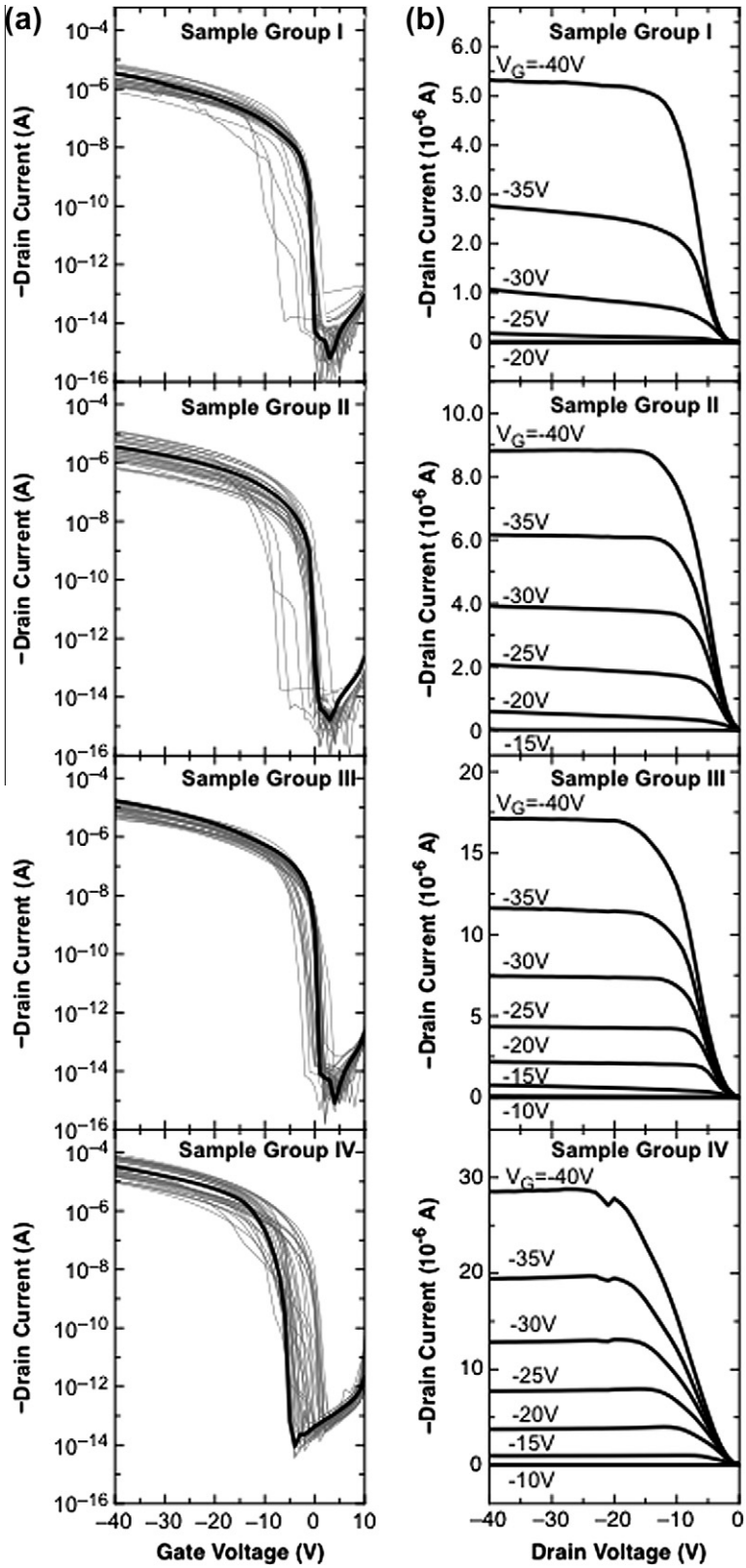

Fig. 6. (a) and (b) Show the transfer and output curves of sample groups I–IV, respectively. In the transfer curves in (a), the gray lines denote all recorded characteristics, and the black lines denote representative curves.

and 0.08 to 0.40 $cm^2\ V^{-1}\ s^{-1}$ when the material concentration decreased from C8-BTBT (1.0 wt.%)/PMMA (2.0 wt.%) to C8-BTBT (0.5 wt.%)/PMMA (0.2 wt.%). Moreover, a typical value of μ_{FET} of the devices in the sample group V with amorphous films was $3.0 \times 10^{-3}\ cm^2\ V^{-1}\ s^{-1}$.

The other outstanding characteristics of organic plate-like transistors are the low V_{th} and small subthreshold swing (S). V_{th} and S are mainly determined by the density and distribution of trap states in the active area of the OFETs [42], and the small values of V_{th} and S for the present devices indicate low trap density at the semiconductor/insulator interface. In particular, S, which manages the voltage swing for a device to operate from off to on, can be applied for the estimation of the maximum trap density (N_{trap}) at the semiconductor/dielectric interface by using the following equation [38,43]:

$$N_{trap} \approx \left[\frac{qS\log(e)}{kT} - 1\right]\frac{C_i}{q}, \tag{2}$$

where q is the electronic charge, k is Boltzmann's constant, and T is the temperature. Using this equation, the interface-trap densities of sample groups I–IV were estimated to be 8.4×10^{11}, 9.9×10^{11}, 9.8×10^{11}, and $1.1 \times 10^{12}\ cm^{-2}$, respectively. The O_2-plasma treatment can introduce hydroxyl groups and fixed interface charges [44]. These values indicate that the PMMA modification of the hydroxyl groups on the SiO_2 layer, which can be attributed to the phase-separation-introduced C8-BTBT/PMMA double layer, reduces trap density. Furthermore, devices from all the sample groups exhibited a very high on/off ratio (10^9–10^{10}), which also suggests that the defect concentration in the crystals and at the active interfaces was limited. Moreover, the FETs based on C8-BTBT plate-like crystals showed good saturation behavior at high drain voltages (V_D) in the output curves (Fig. 6b).

3.5. Measuring the uniformity of device performance

At present, many techniques have been developed for the patterning of organic crystal transistor arrays aimed at simplifying the fabrication processes and achieving better device performance by exhibiting higher mobility. However, the other important issue in the practical applications of patterned organic crystal FETs arrays is the minimization of the variations of performance among devices. High uniformity with small variation is a basic requirement in electronic products such as active matrix backplanes for displays. Aside from the influence of channel traps and metal/semiconductor contact quality, this variation is frequently attributed to the orientation/alignment of crystals and the uniformity of films.

As plotted in Fig. 7, the histograms of μ_{FET}, V_{th}, and S of sample groups I–IV showed uniformity in device performance with different material concentrations. Each sample group had over 30 fabricated devices. From sample groups I–III, better device performance and smaller variation were obtained when the concentration of the

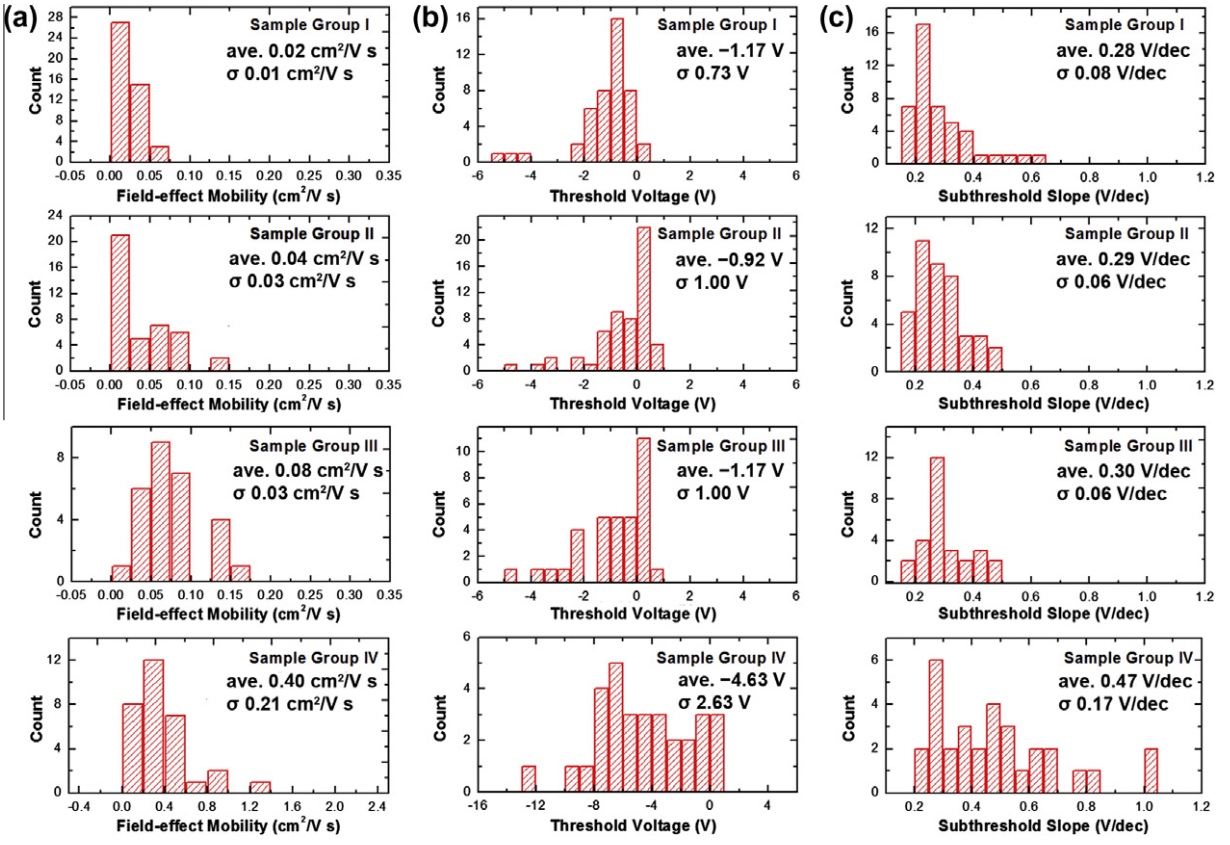

Fig. 7. Histograms of (a) field-effect mobility, (b) threshold voltage, and (c) subthreshold swing of sample groups I–IV.

active materials decreased. In sample III, the average μ_{FET} was 0.08 $cm^2 V^{-1} s^{-1}$, with a standard deviation of 0.03 $cm^2 V^{-1} s^{-1}$. V_{th} and S were -1.17 ± 1.00 V and -0.30 ± 0.06 V/dec, respectively.

The small variations in μ_{FET}, V_{th}, and S enabled the FETs based on the organic plate-like crystals fabricated through the proposed technique to be attractive for use in practical products. When the concentration was further decreased (sample group IV), the average μ_{FET} increased to 0.40 $cm^2 V^{-1} s^{-1}$, with a maximum μ_{FET} of up to 1.25 $cm^2 V^{-1} s^{-1}$. As reported in the literature, μ_{FET} of the organic crystal transistors is frequently influenced by metal/semiconductor contact quality [26,32,45]. Hence, the improvement in μ_{FET} in sample groups I–IV can be attributed to the reduced amount of PMMA covering the crystals when the concentration decreases. However, the variation of the performance in sample IV was larger than that of sample group III. Based on the presented results, high uniformity in performance indicates that the addition of the polymer dielectric to the C8-BTBT solution provides good-film forming characteristics with improved rheology, including viscosity and surface tension. The influence of polymer dielectric on the formation of organic semiconductor films has also been discussed by Ohe et al. for their TIPS-PEN OFETs [46]. Therefore, the relatively poorer uniformity of sample group IV can be attributed to the fact that the lower PMMA concentration resulted in a film with relatively poorer uniformity.

4. Conclusion

In conclusion, a simple approach to pattern the surface wettability using hydrophobic dielectric and to produce plate-like organic crystals within the patterned regions via a direct spin-coating process was demonstrated. C8-BTBT crystals with grain sizes as large as hundreds of micrometers were observed in the patterned regions. By optimizing the material concentrations, the resulting transistors exhibited good device performance and high uniformity, comparable with those of hydrogenated amorphous silicon FETs. The improvement in uniformity can be attributed to the large grain size of the organic semiconductor, which can prevent orientation/alignment-introduced variation, and to the good film uniformity that resulted from the addition of the polymer dielectric to the organic semiconductor solution. The proposed approach is promising for application in the practical production of electronic devices. Also, it is basically applicable to plastic substrates for flexible device, which is currently under investigation.

Acknowledgements

This study is supported partially by the Grand-In-Aid for Scientific Research (No. 218505) from the Ministry of Education, Culture, Sport, Science and Technology of Japan.

References

[1] Z. Bao, J. Locklin, Organic Field-Effect Transistors: Optical Science and Engineering Series, CRC Press, London, 2007.
[2] H. Klauk, Organic Electronics: Materials, Manufacturing, and Applications, Wiley, New York, 2006.
[3] T. Hallam, M. Lee, N. Zhao, I. Nandhakumar, M. Kemerink, M. Heeney, I. McCulloch, H. Sirringhaus, Phys. Rev. Lett. 103 (2009) 256803.
[4] T. Hasegawa, J. Takeya, Sci. Technol. Adv. Mater. 10 (2009) 024314.
[5] R.W.I. de Boer, M.E. Gershenson, A.F. Morpurgo, V. Podzorov, Phys. Status Solidi A 201 (2004) 1302.
[6] J. Takeya, J. Kato, K. Hara, M. Yamagishi, R. Hirahara, Phys. Rev. Lett. 98 (2007) 196804.
[7] H.E. Katz, Chem. Mater. 16 (2004) 4748.
[8] E. Menard, M.A. Meitl, Y.G. Sun, J.U. Park, D.J.L. Shir, Y.S. Nam, S. Jeon, J.A. Rogers, Chem. Rev. 107 (2007) 1117.
[9] Z.N. Bao, J.A. Rogers, H.E. Katz, J. Mater. Chem. 9 (1999) 1895.
[10] D.A. Pardo, G.E. Jabbour, N. Peyghambarian, Adv. Mater. 12 (2000) 1249.
[11] Z.N. Bao, Y. Feng, A. Dodabalapur, V.R. Raju, A.J. Lovinger, Chem. Mater. 9 (1997) 1299.
[12] Z. Wang, J. Zhang, R. Xing, J.F. Yuan, D.H. Yan, Y.C. Han, J. Am. Chem. Soc. 125 (2003) 15278.
[13] C. Kloc, P.G. Simpkins, T. Siegrist, R.A. Laudise, J. Cryst. Growth 182 (1997) 416.
[14] C. Reese, Z.N. Bao, Mater. Today 10 (2007) 20.
[15] J.M. Ball, P.H. Wöbkenberg, F. Colléaux, M. Heeney, J.E. Anthony, D.D.C. Bradley, T.D. Anthopoulos, Appl. Phys. Lett. 95 (2009) 103310.
[16] S.K. Park, T.N. Jackson, J.E. Anthony, D.A. Mourey, Appl. Phys. Lett. 91 (2007) 063514.
[17] K. Takimiya, H. Ebata, K. Sakamoto, T. Izawa, T. Otsubo, Y. Kunugi, J. Am. Chem. Soc. 128 (2006) 12604.
[18] H. Ebata, T. Izawa, E. Miyazaki, K. Takimiya, M. Ikeda, H. Kuwabara, T. Yui, J. Am. Chem. Soc. 129 (2007) 15732.
[19] L. Zhang, C.A. Di, G. Yu, Y.Q. Liu, J. Mater. Chem. 20 (2010) 7059.
[20] C. Liu, T. Minari, X.B. Lu, A. Kumatani, K. Takimiya, K. Tsukagoshi, Adv. Mater. 23 (2011) 523.
[21] S.Y. Park, T. Kwon, H.H. Lee, Adv. Mater. 18 (2006) 1861.
[22] M. Shtein, P. Peumans, J.B. Benziger, S.R. Forrest, J. Appl. Phys. 93 (2003) 4005.
[23] S.C.B. Mannsfeld, A.L. Briseno, S. Liu, C. Reese, M.E. Roberts, Z.N. Bao, Adv. Funct. Mater. 17 (2007) 3545.
[24] A.L. Briseno, J. Aizenberg, Y.J. Han, R.A. Penkala, H. Moon, A.J. Lovinger, C. Kloc, Z.N. Bao, J. Am. Chem. Soc. 127 (2005) 12164.
[25] A.L. Briseno, S.C.B. Mannsfeld, M.M. Ling, S.H. Liu, R.J. Tseng, C. Reese, M.E. Roberts, Y. Yang, F. Wudl, Z.N. Bao, Nature 444 (2006) 913.
[26] S.C.B. Mannsfeld, A. Sharei, S. Liu, M.E. Roberts, Z.N. Bao, Adv. Mater. 20 (2008) 4044.
[27] M. Cavallini, P. Stoliar, J.F. Moulin, M. Surin, P. Leclere, R. Lazzaroni, D.W. Breiby, J.W. Andreasen, M.M. Nielsen, P. Sonar, A.C. Grimsdale, K. Mullen, F. Biscarini, Nano Lett. 5 (2005) 2422.
[28] Q.X. Tang, H.X. Li, Y.B. Song, W. Xu, W.P. Hu, L. Jiang, Y.Q. Liu, X.K. Wang, D.B. Zhu, Adv. Mater. 18 (2006) 3010.
[29] Q.X. Tang, H.X. Li, M. He, W.P. Hu, C.M. Liu, K.Q. Chen, C. Wang, Y.Q. Liu, D.B. Zhu, Adv. Mater. 18 (2006) 65.
[30] T. Minari, M. Kano, T. Miyadera, S.D. Wang, Y. Aoyagi, K. Tsukagoshi, Appl. Phys. Lett. 94 (2009) 093307.
[31] T. Minari, M. Kano, T. Miyadera, S.D. Wang, Y. Aoyagi, M. Seto, T. Nemoto, S. Isoda, K. Kazuhito, Appl. Phys. Lett. 92 (2008) 173301.
[32] Y. Li, C. Liu, A. Kumatani, P. Darmawan, T. Minari, K. Tsukagoshi, AIP Advances. 1 (2011) 022149.
[33] S.H. Liu, W.M. Wang, A.L. Briseno, S.C.B. Mannsfeld, Z.N. Bao, Adv. Mater. 21 (2009) 1217.
[34] A.L. Briseno, M. Roberts, M.M. Ling, H. Moon, E.J. Nemanick, Z.N. Bao, J. Am. Chem. Soc. 128 (2006) 3880.
[35] S.H. Liu, W.M. Wang, S.C.B. Mannsfeld, J. Locklin, P. Erk, M. Gomez, F. Richter, Z.N. Bao, Langmuir 23 (2007) 7428.
[36] H. Minemawari, T. Yamada, H. Matsui, J. Tsutsumi, S. Haas, R. Chiba, R. Kumai, T. Hasegawa, Nature 475 (2011) 364.
[37] H. Sirringhaus, Adv. Mater. 21 (2009) 3859.
[38] S.H. Kim, D. Choi, D.S. Chung, C. Yang, J. Jang, C.E. Park, S.K. Park, Appl. Phys. Lett. 93 (2008) 113306.
[39] T. Endo, T. Nagase, T. Kobayashi, K. Takimiya, M. Ikade, H. Naito, Appl. Phys. Exp. 3 (2010) 121601.
[40] T. Izawa, E. Miyazaki, K. Takimiya, Adv. Mater. 20 (2008) 3388.
[41] S.M. Sze, K.K. Ng, Physics of Semiconductor Devices, third ed., Wiley, New York, 2006.
[42] J. Takeya, T. Nishikawa, T. Takenobu, S. Kobayashi, Y. Iwasa, T. Mitani, C. Goldmann, C. Krellner, B. Batlogg, Appl. Phys. Lett. 85 (2004) 5078.
[43] M. McDowell, I.G. Hill, J.E. McDermott, S.L. Nernasek, J. Schwartz, Appl. Phys. Lett. 88 (2006) 073505.
[44] K. Shin, S.Y. Yang, C. Yang, H. Jeon, C.E. Park, Org. Electron. 8 (2007) 336.
[45] S.D. Wang, Y. Yan, K. Tsukagoshi, Appl. Phys. Lett. 97 (2010) 063307.
[46] T. Ohe, M. Kuribayashi, R. Yasuda, A. Tsuboi, K. Nomoto, K. Satori, M. Itabashi, J. Kasahara, Appl. Phys. Lett. 93 (2008) 053303.